

Luttinger Liquid Physics and Spin-Flip Scattering on Helical Edges

M. Hohenadler¹ and F. F. Assaad^{1,2}

¹*Institut für Theoretische Physik und Astrophysik, Universität Würzburg, Am Hubland, 97074 Würzburg, Germany*

²*Kavli Institute for Theoretical Physics, University of California, Santa Barbara, CA, 93106*

(Dated: July 15, 2021)

We investigate electronic correlation effects on edge states of quantum spin-Hall insulators within the Kane-Mele-Hubbard model by means of quantum Monte Carlo simulations. Given the $U(1)$ spin symmetry and time-reversal invariance, the low-energy theory is the helical Tomanaga-Luttinger model, with forward scattering only. For weak to intermediate interactions, this model correctly describes equal-time spin and charge correlations, including their doping dependence. As apparent from the Drude weight, bulk states become relevant in the presence of electron-electron interactions, rendering the forward-scattering model incomplete. Strong correlations give rise to slowly decaying transverse spin fluctuations, and inelastic spin-flip scattering strongly modifies the single-particle spectrum, leading to graphene-like edge state signatures. The helical Tomanaga-Luttinger model is completely valid only asymptotically in the weak-coupling limit.

PACS numbers: 03.65.Vf, 71.10.Pm, 71.27.+a

Introduction.—A unique feature of quantum spin Hall insulators (QSHIs), or two-dimensional (2D) topological insulators, are metallic edge states with remarkable properties [1]. Contrary to chiral quantum Hall edge states, QSHI edge states are helical, so that electrons with opposite spin propagate in opposite directions. Due to time-reversal invariance (TRI), the helical edge states are protected against disorder and single-particle backscattering [1, 2]. They are also holographic in the sense that they exist only as edges of 2D systems [2], and can therefore not be completely separated from the bulk. The number of pairs of edge states is directly related to the second Chern number or Z_2 invariant [1]. For a review of topological insulators, see Ref. [3].

Quantum fluctuations play a significant role for 2D topological insulators. In particular, the one-dimensional (1D) edges have no well-defined quasiparticle excitations, and are usually described using the framework of bosonization or Luttinger liquid (LL) theory, which becomes particularly simple in the presence of TRI and $U(1)$ spin symmetry. In this case [referred to in the following as the helical Tomanaga-Luttinger (HTL) model], only forward scattering is possible [4]. *A priori*, such a theory is only valid at low energies. Nevertheless, for metallic 1D systems, LL theory provides a complete low-energy description even for strong interactions. For helical edge states, the presence of bulk states is intimately connected with the topological character of the system. Strong interactions on or beyond the size of the bulk band gap can give rise to a substantial mixing of the different energy scales, and may explain deviations of, e.g., the experimentally measured conductance [5] from expectations based on a low-energy description. Bulk effects fall outside the regime of bosonization, and require a model which captures all relevant energy scales. A comparison of the spectral properties of helical, spiral and standard Luttinger liquids has been given in Ref. [6].

The Kane-Mele (KM) model [1] of noninteracting electrons on the honeycomb lattice with spin-orbit (SO) cou-

pling λ is a theoretical framework to study Z_2 QSHIs. For small enough Rashba coupling, the ground state for $\lambda > 0$ is a topological band insulator (TBI). The addition of a Hubbard interaction term (KMH model) permits to study a strongly correlated TBI [7], although it completely detaches the KM model from its original motivation by graphene [8]. The electron-electron interaction leads to a complex and rich many-body problem, which includes a quantum spin liquid phase, and a magnetic transition at large Hubbard U [7, 9–14].

In this Rapid Communication, using large-scale quantum Monte Carlo (QMC) simulations of a previously introduced effective model [9], we provide a comprehensive assessment of the validity of the HTL model. While confirming the interaction and doping dependence predicted for a helical liquid in the weakly interacting limit, we find significant deviations with increasing correlations which are beyond the usual low-energy description and had remained unnoticed in previous numerical work [9, 11, 12]. Additional features in the single-particle spectrum are explained by inelastic spin-flip scattering arising from magnetic fluctuations at the edge, driven by strong electronic correlations. The interaction-driven mixing of multiple energy scales is more subtle than the invalidation of the HTL model due to the breaking of TRI, for example by means of strong bulk interactions [7, 9, 11, 14] which destroy the topological character, or by sufficient renormalization of the LL parameter in the presence of Rashba coupling [2].

Model.—The phase diagram of the KMH model in the $\lambda-U$ plane is known from exact QMC simulations [9, 11, 14]; many of its overall features are also captured by approximate methods [7, 10, 12, 13]. For $U/t \lesssim 3$ (t being the hopping integral), the ground state is a TBI with helical edges for any $\lambda > 0$. The TBI with repulsive $U > 0$ is adiabatically connected to $U = 0$ [9, 14], suggesting that bulk interactions are of minor importance in the TBI phase. Based on this result and the fact that the edge states are exponentially localized at the edge

[9], we have previously proposed an effective model for the helical edge states (which exist throughout the TBI phase) with Hubbard interaction only at one zigzag edge of a semi-infinite honeycomb ribbon. It is defined by the action [9]

$$\mathcal{S} = - \sum_{\sigma, r, r'} \iint_0^\beta d\tau d\tau' c_{r\sigma}^\dagger(\tau) G_0^{\sigma-1}(r - r', \tau - \tau') c_{r'\sigma}(\tau') + U \sum_r \int_0^\beta d\tau [n_{r\uparrow}(\tau) - \frac{1}{2}] [n_{r\downarrow}(\tau) - \frac{1}{2}], \quad (1)$$

where r numbers sites on the zigzag edge, and G_0^σ is the Green's function of the KM model through which the noninteracting bulk is taken into account.

Method.—Equation (1) corresponds to a 1D problem with a bath that can be solved exactly using the continuous-time QMC (CTQMC) method [9, 15] on large systems at low temperatures. Two crucial methodological developments compared to Ref. 9 are the extension to a projective zero-temperature scheme with projection parameter θ , and to grand-canonical simulations away from half filling ($n = 1$). These advances allow for a quantitative test of LL theory. We use the ribbon geometry of [9], with dimensions $L \times L'$ ($L' = 64$), and periodic (open) boundaries in the x (y) direction. The hopping integral and lattice constant are set to 1. The ratio U/λ of the remaining two parameters controls the degree of correlations. To study strong interactions inside the TBI phase of the KM model, we take $U = 2$ and vary λ [9, 14].

Results.—For a zigzag ribbon, the spectral function $A_\sigma(k, \omega) = -\pi^{-1} \text{Im} G_0^\sigma(k, \omega)$ of the $U = 0$ KM model features a bulk energy gap $\Delta_{\text{SO}} \sim 3\sqrt{3}\lambda$ at the Dirac points, and a pair of helical edge states with Fermi velocity $v_F \sim 2\lambda$ crossing at $k_F = \pi$ (for half filling) [1] [see also Fig. 3(a)]. The right (left) movers have spin up (down), and TRI implies $A^\dagger(k, \omega) = A^\dagger(-k, \omega)$. The degeneracy at $k = \pi$ is protected by Kramers' theorem.

Correlation effects on energy scales much smaller than the bulk gap can be studied using bosonization. In the continuum limit, the fermion operator becomes $\Psi_\sigma(r) = e^{ik_F x} \mathcal{R}_\sigma(x) \delta_{\sigma, \uparrow} + e^{-ik_F x} \mathcal{L}_\sigma(r) \delta_{\sigma, \downarrow}$. For a Hubbard interaction, the bosonized Hamiltonian (the HTL model) reads [2, 16, 17]

$$H = \frac{v}{8\pi} \int_0^L dx \left\{ \frac{1}{K} [\partial_x \theta_+(x)]^2 + K [\partial_x \theta_-(x)]^2 \right\}. \quad (2)$$

Here $-\partial_x \theta_\pm(x)/2\pi = \rho_R(x) \pm \rho_L(x)$, with $\rho_R(x)$ and $\rho_L(x)$ being the density of right and left movers, respectively, $v = \sqrt{v_F^2 - (U/2\pi)^2}$ and $K = \sqrt{(v_F - U/2\pi)/(v_F + U/2\pi)}$. Single-particle spin-flip scattering between Kramers degenerate states is blocked by TRI [1, 2, 17]. Umklapp processes such as $e^{i4k_F x} \mathcal{R}^\dagger(x) \mathcal{R}^\dagger(x+a) \mathcal{L}(x) \mathcal{L}(x+a)$ are generally allowed at half filling since $4k_F = 4\pi$, but are forbidden here due to spin- z conservation reflected in the $U(1)$ spin symmetry of the KM model. Hence, only forward scattering

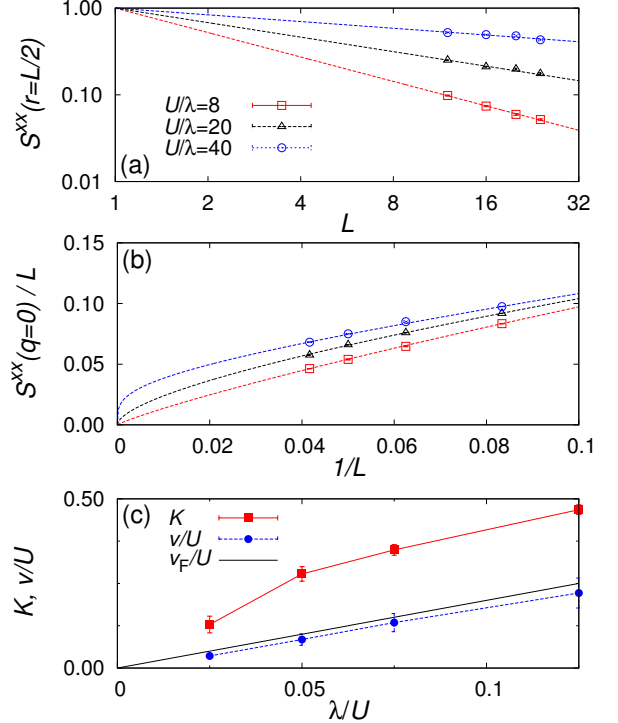


FIG. 1: (Color online) Projective CTQMC results for the effective model (1). (a) Real-space correlations $S^{xx}(r = L/2)$ as a function of system size L at different U/λ , normalized to 1 at $r = 1$ for comparison. The log-log plot reveals a power law with an interaction dependent exponent $\eta = 2K$. (b) $S^{xx}(q = 0)/L$ as a function of $1/L$, demonstrating the absence of long-range order. Lines are fits to the form $S^{xx}(q = 0)/L = b/L + c/L^\eta$, with η taken from (a). Data in (a) and (b) are extrapolated to $\theta = \infty$. (c) Luttinger liquid parameters K and v . K is extracted from fits to the form $S^{xx}(r) = a/r^\eta$ shown as lines in (a). v is estimated from the density structure factor $N(q = 2\pi/L, \tau)$ and finite-size extrapolation; $v_F = 2\lambda$.

is left. The quadratic Hamiltonian (2) gives

$$\begin{aligned} S^{xx}(x) &= \langle S^x(x) S^x(0) \rangle \sim \frac{1}{x^{2K}} \cos(2k_F x), \\ S^{zz}(x) &= \langle S^z(x) S^z(0) \rangle \sim \frac{1}{x^2}, \\ N(x) &= \langle n(x) n(0) \rangle \sim \frac{1}{x^2}. \end{aligned} \quad (3)$$

The transverse correlator $S^{xx}(x)$ involves spin-flip scattering and hence picks up $2k_F$ oscillations in addition to an interaction dependent power-law exponent. $N(x)$ and $S^{zz}(x)$ involve scattering processes only within the left or right movers, and retain their Fermi liquid form. For $K < 1$, transverse spin correlations dominate.

For $U = 0$ ($K = 1$), Eq. (3) can be verified by explicitly solving the effective model of Eq. (1). For $U > 0$, we calculate the correlation functions (3) exactly using QMC, and we show $S^{xx}(r)$ at half filling in Fig. 1(a). With increasing U/λ , we observe a progressively slower decay, corresponding to a reduction of the exponent $2K$.

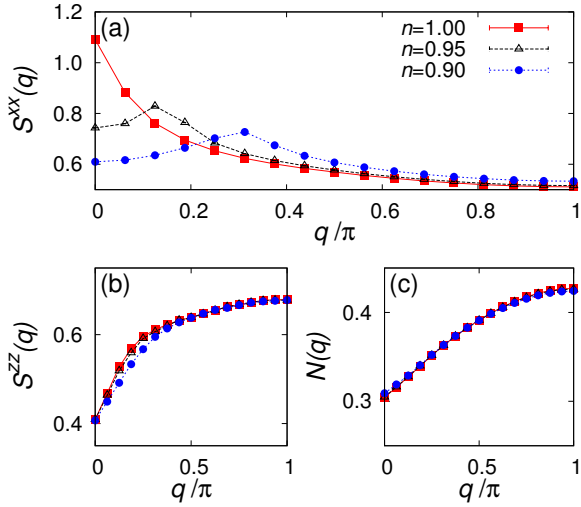


FIG. 2: (Color online) Doping dependence of spin and charge structure factors for $U/\lambda = 8$ from grand-canonical CTQMC simulations ($L = 32$, $\beta = 60$). The $q = 0$ points in (b) and (c) are linear extrapolations.

[see Eq. (3)]. Similar behavior was observed in numerical work [9, 11]. The finite-size scaling of the structure factor $S^{xx}(q = 0)$ shown in Fig. 1(b) confirms the absence of long-range, ferromagnetic order even for $U/\lambda = 40$. This conclusion is based on simulations of very large systems (up to 24×64), whereas smaller sizes would incorrectly suggest long-range order [11, 18]. True (Ising) long-range order becomes possible (at $T = 0$) if the $U(1)$ symmetry of the KMH model is further reduced to Z_2 by Rashba coupling. On the mean-field level, symmetry breaking occurs for any $U > 0$ due to a logarithmic instability.

Figure 1(c) shows the LL parameter K , as obtained from $\eta = 2K$ [Eq. (3)], and the renormalized velocity v calculated from $N(q, \tau)$ (see below). v closely follows the Fermi velocity v_F , with a small offset independent of λ . This result, consistent with v being inherited from the bulk and slightly renormalized by U , conflicts with Eq. (2). We find $K < 1/2$ for the values of U/λ considered, far from the noninteracting limit $K = 1$ and in the regime where umklapp scattering is relevant [2, 11, 18]. However, for translationally invariant systems, this term is allowed only for the special case of exactly half filling and in the presence of Rashba coupling.

The $\cos(2k_F r)$ contribution to $S^{xx}(r)$ becomes apparent upon doping the system by varying the chemical potential inside the bulk gap. As shown in Fig. 2(a) for $U/\lambda = 8$, the peak in the structure factor $S^{xx}(q)$ moves from $q = 0$ to finite q with increasing doping, reflecting the change of k_F . In contrast, the spin- z and charge structure factors retain their cusp structure in the long-wavelength limit related to the $1/r^2$ decay in real space. Deviations from Eq. (3) are observed for $S^{zz}(q)$ outside the long-wavelength limit for large $U/\lambda \gtrsim 10$, and can be related to the strong-coupling effects discussed below.

Figure 3 shows the spectral function $A_\uparrow(k, \omega)$. For

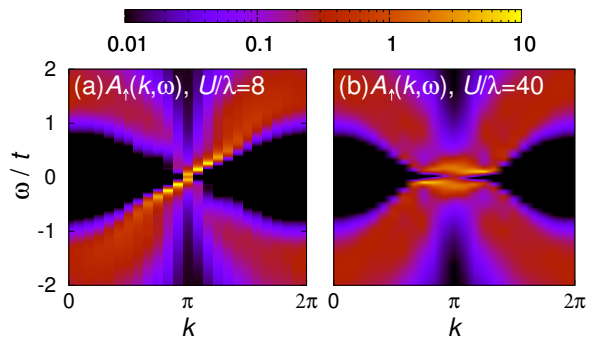


FIG. 3: (Color online) Single-particle spectral function $A_\uparrow(k, \omega)$ from projector-CTQMC simulations for $L = 24$, $\theta = 80$ and (a) $U/\lambda = 8$, (b) $U/\lambda = 40$.

weak coupling [$U/\lambda = 8$, Fig. 3(a)], we see a dominant linear mode crossing the Fermi level, and the spectrum closely resembles the case $U = 0$ [1]. With increasing correlations [$U/\lambda = 40$, Fig. 3(b)], spectral weight is suppressed at low energies in favor of new high-energy features. The spectral function in Fig. 3(b) is fundamentally different from Fig. 3(a) and previous results [9]. The latter were qualitatively fully captured by the HTL model which gives a branch cut $\langle \mathcal{R}^\dagger(x, t) \mathcal{R}(0, 0) \rangle \sim (x - vt)^{-\frac{1}{2}(K+1/K)}$. These additional features arise only in the limit of small spin-orbit coupling (large $U/\lambda \gg 1$).

The HTL model (2) does not account for the single-particle spectrum in Fig. 3(b). Except for the bulk gap at the Dirac points, the locus of spectral weight at high energies near k_F bears remarkable resemblance to the zigzag edge states of graphene ribbons with $U > 0$ [19]. The physics of the latter is dominated by quasi-long-range transverse spin fluctuations at the edge. Similarly, a very slow decay of transverse spin fluctuations at large U/λ [Fig. 1(a)] is a generic signature of the strong-coupling regime of the KMH model, see also Refs. [9, 11].

To identify spin-flip scattering as the physical origin of the high-energy features of Fig. 3(b), we complement our numerical results by a simple yet sufficient analytical approximation. Rewriting the Hubbard term as $H_U = -\frac{1}{2}U \sum_q (S_q^+ S_q^- + S_q^- S_q^+)$ with $S_q^+ = L^{-1/2} \sum_k c_{k\uparrow}^\dagger c_{k+q\downarrow}$, perturbation theory to order U^2 gives the self-energy

$$\Sigma_\uparrow(k, i\omega_m) = \frac{U^2}{\beta L} \sum_{q, i\Omega_m} \chi_0^\pm(q, i\Omega_m) G_0^\downarrow(k - q, i\omega_m - i\Omega_m),$$

with inelastic spin-flip scattering off $q = 2k_F$ transverse spin fluctuations described by the susceptibility $\chi_0^\pm(q, i\Omega_m) = -(\beta L)^{-1} \sum_{k, i\omega_m} G_0^\uparrow(k + q, i\omega_m + i\Omega_m) G_0^\downarrow(k, i\omega_m)$. The results for $A_\uparrow(k, \omega)$ shown in Fig. 4 qualitatively reproduce the numerical data in Fig. 3. For $U/\lambda = 40$, the linear low-energy mode is better visible than in the numerical spectrum whose calculation involves analytical continuation. The emergence of high-

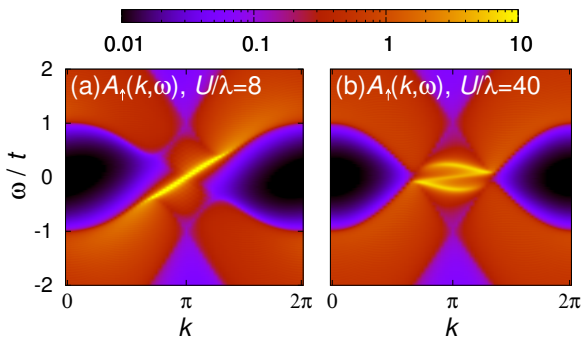


FIG. 4: (Color online) Single-particle spectral function $A_>(k, \omega)$ from second-order perturbation theory. $U/t = 2$.

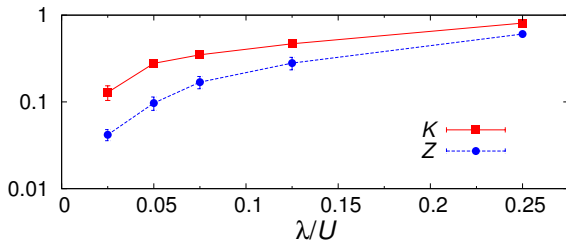


FIG. 5: (Color online) Luttinger parameter K (from Fig. 1) and spectral weight Z from fits to the density structure factor $N(q, \tau)$ at $\theta = 80$ and finite-size scaling. The Luttinger liquid result $K = Z$ is violated for a wide range of parameters.

energy features predominantly above the bulk gap with increasing U/λ causes, via the sum rule $\int d\omega A_\sigma(k, \omega) = 1$, a depletion of spectral weight at low energies. Spin-flip scattering is present for any $U > 0$, but its effects become apparent in $A_>(k, \omega)$ when $U/\lambda \gg 1$.

The deviations from the HTL model and their effect on edge transport may be quantified by measuring the spectral weight Z of low-energy particle-hole excitations using the dynamic charge structure factor $N(q, \omega)$. Fitting the linear mode to the form $N(q, \omega) = \frac{1}{2}Zq\delta(\omega - vq)$, with

weight Z and velocity v estimated from $N(q = 2\pi/L, \tau)$, we can use the continuity equation to obtain the Drude weight $D = Zv$. This result can be compared to the relation $D = Kv$ following from Eq. (2), implying $Z = K$ for the HTL in accordance with results at $U = 0$ (not shown). However, as apparent from the QMC results in Fig. 5, $Z \neq K$ over a wide range of λ/U , and $Z = K$ holds only asymptotically in the weak-coupling limit. Hence, irrespective of the interaction strength, inelastic spin-flip scattering mediated by bulk states leads to deviations from the predictions of the HTL model (2). This effect gains in magnitude with increasing magnetic correlations (increasing U/λ). The suppression of Z (but with $Z = K$) with increasing U/λ (see also Ref. [9]) can be understood in the framework of LL theory. Interaction effects beyond the model (2) are reflected in the pronounced quantitative difference between Z and K .

Conclusions.—Using quantum Monte Carlo simulations, we have investigated the validity of the low-energy Tomanaga-Luttinger model for edge states of a Z_2 topological insulator. We found the expected interaction and doping dependence of spin and charge correlations, with dominant transverse spin fluctuations but no long-range order. However, the fact that helical edge modes cannot strictly be energetically separated from the insulating bulk has important consequences. The bulk states provide phase space for inelastic spin-flip scattering. In the weak-coupling limit, this leads to minor but quantifiable violations from bosonization predictions. For strong coupling, these scattering processes transfer spectral weight from low to high energies in the single-particle spectral function, and thereby give rise to features reminiscent of graphene zigzag ribbons.

We thank J. Budich, T. Lang, Z. Y. Meng, P. Recher, M. Schmidt, T. Schmidt, B. Trauzettel, S.-C. Zhang and C. Xu for discussions. This research was supported in part by the National Science Foundation under Grant No. PHY05-51164. We acknowledge support from DFG Grant No. FOR1162 and generous computer time at the LRZ Munich and the Jülich Supercomputing Centre.

[1] C. L. Kane and E. J. Mele, Phys. Rev. Lett. **95**, 146802 (2005).
[2] C. Wu, B. A. Bernevig, and S.-C. Zhang, Phys. Rev. Lett. **96**, 106401 (2006).
[3] M. Z. Hasan and C. L. Kane, Rev. Mod. Phys. **82**, 3045 (2010).
[4] T. Giamarchi, *Quantum Physics in One Dimension* (Clarendon Press, Oxford, 2004).
[5] M. König, S. Wiedmann, C. Brüne, A. Roth, H. Buhmann, L. W. Molenkamp, X.-L. Qi, and S.-C. Zhang, Science **318**, 766 (2007).
[6] B. Braunecker, C. Bena, and P. Simon, Phys. Rev. B **85**, 035136 (2012).
[7] S. Rachel and K. Le Hur, Phys. Rev. B **82**, 075106 (2010).
[8] C. L. Kane and E. J. Mele, Phys. Rev. Lett. **95**, 226801 (2005).
[9] M. Hohenadler, T. C. Lang, and F. F. Assaad, Phys. Rev. Lett. **106**, 100403 (2011).
[10] Y. Yamaji and M. Imada, Phys. Rev. B **83**, 205122 (2011).
[11] D. Zheng, G.-M. Zhang, and C. Wu, Phys. Rev. B **84**, 205121 (2011).
[12] S.-L. Yu, X. C. Xie, and J.-X. Li, Phys. Rev. Lett. **107**, 010401 (2011).
[13] W. Wu, S. Rachel, W.-M. Liu, and K. Le Hur, arXiv:1106.0943 (2011).
[14] M. Hohenadler, Z. Y. Meng, T. C. Lang, S. Wessel, A. Muramatsu, and F. F. Assaad, arXiv:1111.3949 (2011).
[15] A. N. Rubtsov, V. V. Savkin, and A. I. Lichtenstein, Phys. Rev. B **72**, 035122 (2005).

- [16] N. Nagaosa, *Quantum Field Theory in Strongly Correlated Electronic Systems* (Springer, Berlin, 1999).
- [17] C. Xu and J. E. Moore, Phys. Rev. B **73**, 045322 (2006).
- [18] D.-H. Lee, Phys. Rev. Lett. **107**, 166806 (2011).
- [19] H. Feldner, Z. Y. Meng, T. C. Lang, F. F. Assaad, S. Wessel, and A. Honecker, Phys. Rev. Lett. **106**, 226401 (2011).